

# Center motions of nonoverlapping condensates coupled by long-range dipolar interaction in bilayer and multilayer stacks

Chao-Chun Huang and Wen-Chin Wu

*Department of Physics, National Taiwan Normal University, Taipei 11650, Taiwan*

We investigate the effect of anisotropic and long-range dipole-dipole interaction (DDI) on the center motions of nonoverlapping Bose-Einstein condensates (BEC) in bilayer and multilayer stacks. In the bilayer, it is shown analytically that while DDI plays no role in the in-phase modes of center motions of condensates, out-of-phase mode frequency ( $\omega_o$ ) depends crucially on the strength of DDI ( $a_d$ ). At the small- $a_d$  limit,  $\omega_o^2(a_d) - \omega_o^2(0) \propto a_d$ . In the multilayer stack, transverse modes associated with center motions of coupled condensates are found to be optical phonon like. At the long-wavelength limit, phonon velocity is proportional to  $\sqrt{a_d}$ .

PACS numbers: 03.75.Hh, 03.65.-w

## I. INTRODUCTION

In contrast to the isotropic  $s$ -wave contact interaction, dipole-dipole interaction (DDI) has a very distinct character – anisotropic and long-range. This character results in various interesting phenomena in ultracold dipolar atom or molecule systems. The studies of DDI effect on the structure and dynamics of quantum many-body systems is at the forefront of both theoretical and experimental interests. In recent years dipolar chromium ( $^{52}\text{Cr}$ ) atoms were created with a magnetic moment of  $6\mu_B$  ( $\mu_B$  is Bohr magneton), which is equivalent to a dipole moment  $d \approx 0.056D$  ( $1D \simeq 3.335 \times 10^{-30}\text{C}\cdot\text{m}$ ) [1]. More recently, creations of dipolar molecules have also been achieved in ultracold heteronuclear molecules such as  $^{40}\text{K}^{87}\text{Rb}$  with a much stronger dipole moment  $d \approx 0.6D$  [2, 3]. From the theoretical point of view, many interesting physical properties have been studied, such as biconcave shapes of the ground state [4–6], intriguing collapse mechanisms [5, 7–10], vortex structures [11–13], anisotropic solitons [14] and so on.

Among many others, properties of *nonoverlapping* dipolar Bose-Einstein condensates (BEC) in bilayer or multilayer (quasi-1D optical lattice) stacks have attracted great attention in recent years. The topics under investigation include phonon instability [15, 16], soliton-soliton scattering [17], pair superfluidity [18], and filament condensation [19]. In these systems, condensates are effectively nonoverlapping between neighboring layers and as a matter of fact, contact or even short-range interaction plays no role between neighboring layers. However, long-range DDI will still play an important role across different layers. Moreover in a real system, dipoles of the dipolar gas are usually aligned (by applying strong electric or magnetic field) along the direction of the stacks. This in turn will make dipolar molecular systems more stable against recombination and result in better opportunity of forming dipolar molecular BEC.

This paper attempts to study collective excitations of nonoverlapping atomic or molecular BEC in bilayer and multilayer stacks, that are coupled by long-range DDI. The focus will be placed on the motions of the *centers*

of condensates. When weakly interacting Bose condensates are loaded into a single harmonic (magnetic) trap, it is well known that, for small oscillations, center motion of condensates will undergo harmonic oscillation of frequency equal to the characteristic trap frequency [20, 21]. This remains true even when the system has a long-range DDI in it. When condensates are loaded into a double well and form a bilayer system in, say,  $z$  direction (while a single harmonic trap is applied in the  $x$ - $y$  plane), center motions of the two condensate clouds can be very interesting upon the activation of long-range DDI. It will be shown explicitly that when DDI is present, both in-phase and out-of-phase motions of the two condensate centers will still undergo harmonic oscillations (for small oscillations). However, while in-phase modes are independent of DDI, out-of-phase modes will depend crucially on the strength of DDI.

In addition, it is also interesting to investigate center motions of nonoverlapping condensates in a multilayer stack (quasi-1D optical lattice along  $z$ -direction). By properly treating the boundary effect (see later), transverse modes associated with motions of the centers of condensates in each layer are found to be optical phonon like. At infinitely long wavelength limit ( $q_z \rightarrow 0$ ), phonon mode frequency just equals to the harmonic trap frequency in the  $x$ - $y$  plane and at the long-wavelength limit ( $q_z z_0 \ll 1$ ,  $z_0$  is the lattice constant), phonon mode velocity is found to be proportional to the square root of the strength of DDI. Due to the long-range character of DDI, for the multilayer system of finite number of layers, it is important to treat properly the boundary effect. With this regard, we have introduced a truncation number ( $N_c^g$ ) which corresponds to number of neighboring layers included for satisfactorily converged results. It is found that  $N_c^g$  will depend on the ratio of lattice constant ( $z_0$ ) and condensate radius in the  $x$ - $y$  plane only.

To end this introductory section, we emphasize two things. Firstly, the results presented in this paper, especially the dependence of DDI strength on center motion mode frequencies, are believed to be valid even when the system is not Bose condensed. Since long-range DDI survives in the non-condensed system, it is encouraging

that the experiment can also be done on the ultracold heteronuclear dipolar molecules which exhibits a strong dipole moment but nevertheless is yet to be Bose condensed [2, 3]. Secondly, the strength of DDI can actually be extracted through measurements of out-of-phase mode in the bilayer or transverse phonon mode in the multilayer stack.

The paper is organized as the following. In Sec. II, energy functional of a nonoverlapping bilayer system is given. Proper trial wave functions are introduced within the variational framework and minimized ground-state energies are obtained. In Sec. III, analytical results of the mode frequency for center motions of condensates are given. It is shown that while in-phase mode frequency is independent of the strength of DDI, out-of-phase modes depend crucially on the strength of DDI. In Sec. IV, we extend the study to the center motions of condensates in a multilayer stack. By properly treating the boundary effect, transverse phonon modes are obtained. At the long-wavelength limit, we show that phonon velocity is proportional to the square root of the strength of DDI. Sec. V is a conclusion.

## II. NONOVERLAPPING BILAYER SYSTEM

We consider a nonoverlapping bilayer system with same BEC atoms or molecules in each layer. Energy functional of the system is given by

$$E = E_1 + E_2 + E_{12}, \quad (1)$$

where ( $i = 1, 2$ )

$$E_i = N \int d\mathbf{r} \psi_i^*(\mathbf{r}) \left[ -\frac{\hbar^2}{2m} \nabla^2 + V_{\text{ext},i}(\mathbf{r}) \right] \psi_i(\mathbf{r}) + \frac{N-1}{2} \left( g |\psi_i(\mathbf{r})|^2 + \int d\mathbf{r}' V_{dd}(\mathbf{r} - \mathbf{r}') |\psi_i(\mathbf{r}')|^2 \right) \quad (2)$$

and

$$E_{12} = N^2 \int \int d\mathbf{r} d\mathbf{r}' V_{dd}(\mathbf{r} - \mathbf{r}') |\psi_1(\mathbf{r})|^2 |\psi_2(\mathbf{r}')|^2. \quad (3)$$

Here  $E_1$  and  $E_2$  correspond to intralayer energies and  $E_{12}$  is the interlayer energy caused by DDI.  $N$  is the number of condensed atoms or molecules in each layer and  $\psi_i$  is the normalized wave function for layer  $i$ .  $g = 4\pi\hbar^2 a/m$  with  $a$  the  $s$ -wave scattering length and  $V_{dd}(\mathbf{r}) = d^2(1 - 3\cos^2\theta)/|\mathbf{r}|^3$  is the dipole-dipole interaction with  $\theta$  the angle between  $\mathbf{r}$  and the dipole orientation. For magnetic dipoles, the strength  $d^2 = \mu_0\mu_m^2/4\pi$  with  $\mu_m$  the magnetic dipole moment, while for electric dipoles,  $d^2 = d_e^2/4\pi\epsilon_0$  with  $d_e$  the electric dipole moment. For a nonoverlapping bilayer considered in current context, condensate wave functions are not overlapped across the two layers, *i.e.*,  $\int d\mathbf{r} |\psi_1(\mathbf{r})|^2 |\psi_2(\mathbf{r})|^2 \approx 0$ . As a consequence, interlayer energies associated with  $s$ -wave interaction as well as interlayer hopping are neglected.

To create a nonoverlapping bilayer ultracold BEC system, one can set up a double well with a large barrier in the middle. One possible candidate of nonoverlapping double potential well in  $z$  direction is  $V = \frac{1}{2}m(\omega_x^2 x^2 + \omega_y^2 y^2 + \omega_z^2 z^2) + V_\ell \cos^2(\pi z/d_\ell)$  by applying a harmonic trap together with a deep optical (lattice) trap [22]. Alternatively, one can apply a harmonic trap together with a repulsive barrier potential to obtain  $V = \frac{1}{2}m(\omega_x^2 x^2 + \omega_y^2 y^2 + \omega_z^2 z^2) + V_0 \exp(-z^2/\ell_z^2)$  [23]. By controlling the values of  $V_\ell$  *vs.*  $d_\ell$  or  $V_0$  *vs.*  $\ell_z$ , effective nonoverlapping bilayer system can be formed. As a matter of fact, wave function of each layer is extremely narrow (pancake like) in  $z$ -direction and to the leading order, trap potentials experienced by the atoms or molecules in each layer can be approximated by the following anisotropic harmonic potentials,

$$V_{\text{ext},1,2}(\mathbf{r}) = \frac{1}{2}m \left[ \omega_x^2 x^2 + \omega_y^2 y^2 + \omega_z^2 (z \mp z_1/2)^2 \right]. \quad (4)$$

Here  $z_1$ , determined by the experimental setup, corresponds to the spacing between the two trap minima located at  $z = \pm z_1/2$ . For nonoverlapping bilayer systems,  $\omega_z$  is typically much larger than  $\omega_x$  and  $\omega_y$ . In this paper, as depicted in Fig. 1, we consider the dipolar system to which dipoles are oriented along  $z$  direction. With this geometry, the system will be the most stable compared to others.

Within the variational framework, Gaussian ansatz is used for the trial wave functions of the bilayer system. As long as the system is not close to a collapsed state, Gaussian function should be a good trial wave function for the system [24]. For layer 1 and 2, we then take

$$\psi_{1,2}(\mathbf{r}) = A \exp \left[ -\frac{1}{2} \left( \frac{x^2}{R_x^2} + \frac{y^2}{R_y^2} + \frac{(z \mp z_0/2)^2}{R_z^2} \right) \right], \quad (5)$$

where variational parameters  $R_x$ ,  $R_y$ , and  $R_z$  correspond to condensate radii in  $x$ ,  $y$ , and  $z$  directions,  $A = 1/\sqrt{R_x R_y R_z \pi^{3/2}}$  is the normalization constant, and  $z_0$  corresponds to the distance between the two condensate centers located at  $z = \pm z_0/2$ . Note in general that  $z_0$  can be different from  $z_1$  [the latter corresponds to trap minima, see Eq. (4)]. When DDI vanishes,  $z_0$  will be identical to  $z_1$ . However, when DDI is present,  $z_0$  will be smaller (larger) than  $z_1$  if DDI is attractive (positive) in  $z$  direction. Nevertheless, for the present nonoverlapping bilayer system,  $z_0$  should be not much different from  $z_1$ .

Truly speaking, due to anisotropic nature of DDI, real wave function for each layer will not be symmetric in  $z$  direction even though a symmetric potential trap (4) is in effect. However, when  $\omega_z \gg \omega_x, \omega_y$ , wave function in each layer is still relatively symmetric in  $z$  direction. Substituting trial wave functions (5) and trap potentials (4) into energy functional (1)–(3), we obtain

$$E = N \left\{ \frac{1}{2R_x^2} + \frac{1}{2R_y^2} + \frac{1}{2R_z^2} + \lambda_z^2 \left[ \frac{R_z^2}{2} + \frac{(z_0 - z_1)^2}{4} \right] \right\}$$

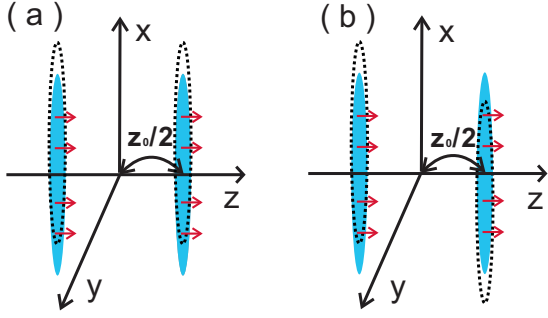


FIG. 1. Sketch of the nonoverlapping bilayer condensates and their center motions along the  $x$ -direction. Red arrows denote the direction of dipoles. Blue stacks represent the stationary condensates, while black dash lines represent their movements. Frame (a) corresponds to the in-phase mode and frame (b) corresponds to the out-of-phase mode.

$$+ \frac{R_x^2}{2} + \lambda_y^2 \frac{R_y^2}{2} + \frac{N-1}{R_x R_y R_z} \left( \sqrt{\frac{2}{\pi}} a_s - a_d F_0 \right) \left\{ - \frac{N^2}{R_x R_y R_z} a_d F. \right. \quad (6)$$

In (6) and throughout this paper, we have rescaled the energy  $E/(\hbar\omega_x) \rightarrow E$  and the time  $t\omega_x \rightarrow t$ . Besides, all the lengths ( $R_x, R_y, R_z, z_0, z_1$ ) are scaled by the magnetic length in  $x$ -direction,  $\ell \equiv \sqrt{\hbar/m\omega_x}$ , and the ratios  $\lambda_y \equiv \omega_y/\omega_x$  and  $\lambda_z \equiv \omega_z/\omega_x$ . Dimensionless coupling strength  $a_d \equiv d^2 m/\hbar^2 \ell$  and  $a_s \equiv a/\ell$ .  $F = F(z_0, R_x, R_y, R_z)$  is related to the interlayer energy due to DDI, while  $F_0 \equiv F(z_0 = 0, R_x, R_y, R_z)$  is related to the intralayer energy due to DDI. More explicitly, for dipoles aligned along the  $z$  direction,  $F$  is given by the following integral

$$F = \frac{1}{6\pi^2} \int d\mathbf{k} \exp \left[ -\frac{1}{2} (k_x^2 + k_y^2 + k_z^2) \right] \cos \left( k_z \frac{z_0}{R_z} \right) \times \left( 1 - \frac{3k_z^2}{k_x^2 R_z^2/R_x^2 + k_y^2 R_z^2/R_y^2 + k_z^2} \right). \quad (7)$$

Values of  $R_x, R_y, R_z$ , and  $z_0$  for the ground state are obtained by solving the conditions  $\partial E/\partial R_i = 0$  ( $i = x, y, z$ ) and  $\partial E/\partial z_0 = 0$ .

### III. CENTER MOTIONS OF BILAYER SYSTEM

As mentioned before, in this paper we focus on the motions of the center of condensates along  $x$  direction (see Fig. 1). Generalization to considering as well the center motions of condensates along  $z$  direction is straightforward. However, for condensates strongly confined in  $z$  direction, condensate wave functions are rigid in  $z$  direction and as a consequence collective excitation in  $z$  direction will cost more energy. Besides observation of these motions of much smaller amplitude are relatively more difficult.

By variational approach, suitable dynamical variables should be added into the trial wave functions (5). In Ref. [20, 21], it was shown in the single-trap system that equations of motion for the center of condensates are decoupled from equations of motion for the width of condensates. For a bilayer system studied in this context, similar decoupling occurs although the proof is omitted for brevity. As a matter of fact, for the motions of the center of condensates, dynamical wave functions can be taken to be

$$\psi_{1,2}(\mathbf{r}, t) = A \exp \left[ -\frac{y^2}{2R_y^2} - \frac{(z \mp z_0/2)^2}{2R_z^2} \right] \times \exp \left\{ -\frac{[x - x_{1,2}(t)]^2}{2R_x^2} - i x c_1(t) \right\}, \quad (8)$$

where dynamical variables are added associated with the center motions only. Here  $x_i(t)$  corresponds to the fluctuation of the center of condensate of layer  $i$  in  $x$ -direction, while  $c_i(t)$  corresponds to the sloping phases of the condensates of layer  $i$ . The task is to find the equations of motion and solve it.

We start from the effective Lagrangian,  $L = T + E$ , where  $T$  is given by

$$T = \int d\mathbf{r} \sum_{j=1,2} N \left( \frac{i\hbar}{2} \right) \left[ \psi_j \frac{\partial \psi_j^*}{\partial t} - \psi_j^* \frac{\partial \psi_j}{\partial t} \right] \quad (9)$$

and  $E$  is given by Eqs. (1)–(3). Substituting Eq. (8) into the Lagrangian and expanding dynamical variables up to second order (for small oscillations), one obtains

$$L = \sum_{i=1,2} N \left( \frac{x_i^2}{2} + \frac{c_i^2}{2} - x_i \dot{c}_i \right) + \frac{N^2 a_d G (x_1 - x_2)^2}{2R_x^3 R_y R_z} \quad (10)$$

where  $G = G(z_0, R_x, R_y, R_z)$  and given by the integral

$$G = \frac{1}{6\pi^2} \int d\mathbf{k} k_x^2 \exp \left[ -\frac{1}{2} (k_x^2 + k_y^2 + k_z^2) \right] \cos \left( k_z \frac{z_0}{R_z} \right) \times \left( 1 - \frac{3k_z^2}{k_x^2 R_z^2/R_x^2 + k_y^2 R_z^2/R_y^2 + k_z^2} \right). \quad (11)$$

It is interesting to note that  $s$ -wave scattering coupling  $a_s$  has completely dropped out in  $L$  in (10). Equations of motion can be derived using the Lagrange equation,  $\frac{d}{dt} \frac{\partial L}{\partial \dot{q}} = \frac{\partial L}{\partial q}$ , where  $q$  can be any one of the four dynamical variables. By assuming  $q = q_0 \exp(i\omega t)$ , after some algebra we obtain two branches of excitation modes:

$$\omega_i^2 = 1, \quad \omega_o^2 = 1 + N a_d \left( \frac{2G}{R_x^3 R_y R_z} \right), \quad (12)$$

where  $\omega_i$  corresponds to the in-phase mode associated with the solutions of  $x_1 = x_2$  and  $c_1 = c_2$  [such as the motion depicted in Fig. 1(a)]. While  $\omega_o$  corresponds to the out-of-phase mode associated with the solutions of  $x_1 = -x_2$  and  $c_1 = -c_2$  [such as the motion depicted in Fig. 1(b)].

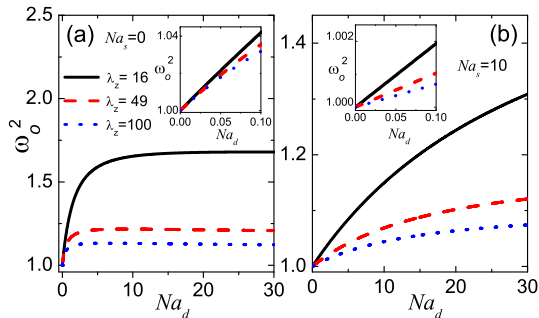


FIG. 2. The square of out-of-phase mode,  $\omega_o^2$ , plotted as the function of  $Na_d$  ( $N$  is particle number in each layer and  $a_d$  is DDI coupling) for  $\lambda_z = 16, 49$ , and  $100$  respectively. The insets show linear dependence of  $Na_d$  at small  $Na_d$ . In frame (a),  $s$ -wave coupling  $Na_s = 0$  and in frame (b),  $Na_s = 10$ .  $z_1$  is chosen to be  $1.2\ell$  in both frames.

Since  $x$ -direction harmonic trap frequency  $\omega_x$  is the energy unit used in this context, the results in (12) show that in-phase mode frequency of  $x$ -direction center motions of bilayer condensates is just  $\omega_x$ , independent of the long-range DDI. For the out-of-phase mode, in contrast, the mode frequency is shifted from  $\omega_x$  and the deviation depends crucially on the strength of DDI ( $a_d$ ). To be more explicitly, the deviation will depend on  $a_d$ , the number  $N$ , as well as the four lengths ( $R_x, R_y, R_z, z_0$ ). Since number  $N$  and the four lengths are measurable quantities, one can then calculate  $G$  [using Eq. (11)] with the measured values of  $N$  and ( $R_x, R_y, R_z, z_0$ ). This simply means that once center motions of the bilayer is performed and out-of-phase mode frequency  $\omega_o$  is measured, one can actually extract the value of  $a_d$  via Eq. (12).

Fig. 2 shows the square of out-of-phase mode  $\omega_o^2$  as the function of  $Na_d$ . For convenience, we consider the isotropic case in  $xy$  plane ( $R_x = R_y \equiv R$  and  $\lambda_y = 1$ ), and have chosen  $z_1 = 1.2\ell$ . Fig. 2(a) plots the  $Na_s = 0$  case with  $\lambda_z$  chosen to be 16, 49, and 100 respectively. While Fig. 2(b) plots  $Na_s = 10$  case with the same choice of the three  $\lambda_z$ 's. The insets show the linear dependence of  $Na_d$  when  $Na_d$  is small. Within variational framework, values of  $R$ ,  $R_z$ , and  $z_0$  are determined by minimizing the energy functional (6). It is useful to check that when both  $s$ -wave and DDI couplings are absent,  $a_s = a_d = 0$ , one finds that  $z_0 = z_1$ ,  $R = 1\ell$ , and  $R_z = (1/4)\ell$ ,  $(1/7)\ell$ , and  $(1/10)\ell$  corresponding respectively to  $\lambda_z = 16, 49$  and  $100$  cases. However, when  $a_d$  is present,  $z_0$  becomes shorter than  $z_1$ , while  $R$  and  $R_z$  become larger than those for the case of  $a_d = 0$ . This simply means that the ratio of  $z_0/R_z$  will become smaller in the presence of  $a_d$ . Nevertheless, in the strong confining regime ( $z_0/R_z \geq 4$ ) considered in this context, the change of  $z_0/R_z$  due to  $a_d$  is minor. For example, in case of  $a_s = 0$  and  $Na_d = 30$ , ratio  $z_0/R_z$  is found to be 4.07, 7.9, and 11.6 for  $\lambda_z = 16, 49$  and  $100$ , as compared to 4.8, 8.4, and 12 for the case of  $a_s = a_d = 0$ .

When results of Fig. 2(b) are compared to those in

Fig. 2(a), one sees that repulsive  $s$ -wave coupling  $a_s$  acts to reduce the deviation of  $\omega_o$  from  $\omega_x$ . While short-range  $a_s$  plays no role between neighboring layers, its repulsion actually increases the radii of condensate ( $R_x, R_y, R_z$ ) in each layer and consequently  $G/R_x^3 R_y R_z$  becomes smaller. This indicates that  $\omega_o^2$  or its slope against  $Na_d$  (at small  $Na_d$ ) will be smaller. In addition, it is found that regardless of the value of  $a_s$ , for the same  $Na_d$ , the larger  $\lambda_z$  is, the closer  $\omega_o$  is to  $\omega_x$ . In  $^{52}\text{Cr}$  atom dipolar BEC, it has been measured that  $d^2 m/\hbar^2 \simeq 24 \text{ \AA}$ . If atom number in one layer is  $N \sim 10^4$  and the harmonic oscillator length  $\ell \sim 1 \mu\text{m}$ , then it is estimated that  $Na_d \sim 20$ . This gives a reference how large  $\omega_o$  is when the results of Fig. 2 are considered.

#### IV. NONOVERLAPPING MULTILAYER STACK

In this section, we extend to study center motions of condensates in a multilayer stack. As before, condensates are assumed to be non-overlapping between neighboring layers. The kind of system can be realized in a deep quasi-1D optical lattice [25]. In an analogous way, energy functional of the multilayer system can be given by

$$E = \sum_{n=1}^{N_s} \left( E_n + \sum_m E_{n,m} \right), \quad (13)$$

where

$$E_n = N \int d\mathbf{r} \psi_n^*(\mathbf{r}) \left[ -\frac{\hbar^2}{2m} \nabla^2 + V_{\text{ext}}(\mathbf{r}) + \frac{N-1}{2} \left( g|\psi_n(\mathbf{r})|^2 + \int d\mathbf{r}' V_{dd}(\mathbf{r}-\mathbf{r}') |\psi_n(\mathbf{r}')|^2 \right) \right] \psi_n(\mathbf{r}) \quad (14)$$

and

$$E_{n,m} = N^2 \int \int d\mathbf{r} d\mathbf{r}' V_{dd}(\mathbf{r}-\mathbf{r}') |\psi_n(\mathbf{r})|^2 |\psi_{n+m}(\mathbf{r}')|^2 \quad (15)$$

Here  $N_s$  corresponds to the number of layers in the stack and  $N$  corresponds to the number of atoms in each layer.  $E_n$  represents the intralayer energy for layer  $n$ , while  $E_{n,m}$  represents the interlayer energy between layers  $n$  and  $(n+m)$  coupled by DDI. The external trap,  $V_{\text{ext}}$ , consists of magnetic and optical traps, where magnetic trap is  $m(\omega_x^2 x^2 + \omega_y^2 y^2)/2$ , while optical trap is  $sE_r \sin^2(\pi z/z_0)$  with  $z_0$  the spacing between neighboring layers,  $s$  the strength of optical trap, and  $E_r = \hbar^2 \pi^2 / 2mz_0^2$  the recoil energy.

In the calculation, we shall use the following approximation for  $E$  in Eq. (13):

$$E \simeq \sum_{n=1}^{N_s} \left( E_n + \sum_{|m|=1}^{N_c} E_{n,m} \right), \quad (16)$$

where  $N_c$  is a truncation number to which how many neighboring sites are included for  $E_{n,m}$  ( $|m| = 1$  correspond to the two nearest neighbors). With (16), periodic

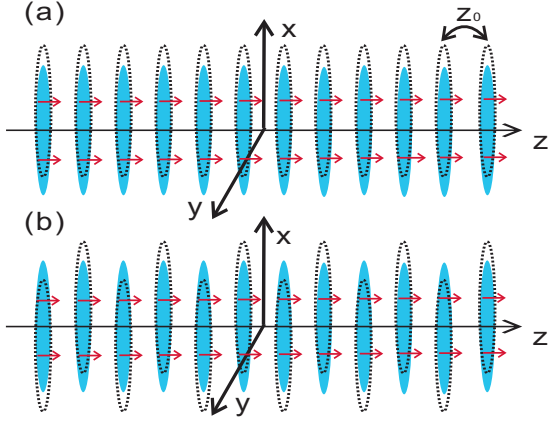


FIG. 3. Sketch of the multilayer stack and the motions of the center of condensates. Frame (a) corresponds to a  $q_z = 0$  in-phase phonon mode and frame (b) corresponds to a  $q_z = \pi/z_0$  out-of-phase phonon mode. Red arrows denote the direction of dipoles. Blue stacks represent the stationary condensates and black dash lines represent the motions of condensates.

boundary condition (PBC) which connects the two ends is applied. Owing to the long-range nature of DDI, it is expected that for a satisfactory converged result,  $N_c \gg 1$ . On the other hand, for a trusty result, it is required that the truncation number should be much smaller than the total number of layers in the stack ( $N_c \ll N_s$ ).

In the current multilayer stack, for simplicity, we also apply the Gaussian ansatz for the trial wave function of each layer [similar to that of Eq. (5)]. It should be emphasized again that due to the boundary effect, true wave function associated with each layer is not perfectly symmetric in  $z$  direction. Nevertheless, for the current nonoverlapping condensates under study, a symmetric wave function will be a good approximation for each layer. After a lengthy derivation, we obtain the following energy functional for the multilayer system

$$\begin{aligned} \frac{E}{N_s} = N \left\{ \frac{1}{4R_x^2} + \frac{1}{4R_y^2} + \frac{1}{4R_z^2} + \frac{sE_r}{2}(1 - e^{-\pi^2 R_z^2/z_0^2}) \right. \\ \left. + \frac{R_x^2}{4} + \lambda_y^2 \frac{R_y^2}{4} + \frac{N-1}{2R_x R_y R_z} \left( \sqrt{\frac{2}{\pi}} a_s - a_d F_0 \right) \right\} \\ - \frac{N^2 a_d}{2R_x R_y R_z} \Gamma(N_c), \end{aligned} \quad (17)$$

where

$$\Gamma(N_c) \equiv \sum_{|m|=1}^{N_c} F_m \quad (18)$$

with  $F_m$  being just  $F$  in Eq. (7) with  $\cos(k_z z_0/R_z)$  term replaced by  $\cos(mk_z z_0/R_z)$ . Once again, it is assumed that dipoles of the dipolar gas are aligned along the  $z$ -direction and we consider only the motions of the center of condensates in  $x$  direction for small oscillations (see Fig. 3). In (17), all energies and lengths are rescaled in the same way as those in the bilayer case. The recoil

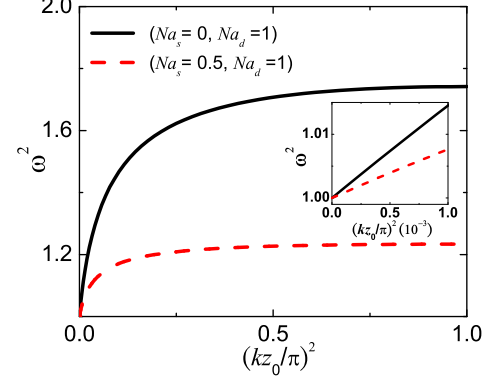


FIG. 4. Square of the transverse phonon modes plotted as the function of  $(kz_0/\pi)^2$ . Two cases,  $(Na_s, Na_d) = (0, 1)$  and  $(0.5, 1)$  are presented. The inset shows the linearity at long wavelength limit ( $kz_0 \ll \pi$ ) and the slope is equal to the square of phonon velocity.

energy will then reduce to  $E_r = \pi^2 \ell^2 / 2z_0^2$  in the dimensionless unit.

With the same variational approach, we obtain the Lagrangian of the system (keeping dynamical variables up to second order)

$$\begin{aligned} L = N \sum_n \left[ \frac{x_n^2}{2} + \frac{c_n^2}{2} - x_n \dot{c}_n \right. \\ \left. + \sum_{|m|=1}^{N_c} \frac{Na_d (x_n - x_{n+m})^2}{4R_x^3 R_y R_z} G_m \right] \end{aligned} \quad (19)$$

with  $G_m$  being just  $G$  in Eq. (11) with  $\cos(k_z z_0/R_z)$  term replaced by  $\cos(mk_z z_0/R_z)$ . Similar to those in Eq. (8), dynamical variable  $x_n = x_n(t)$  corresponds to the fluctuation of the center of condensate of layer  $n$  in  $x$ -direction, while  $c_n = c_n(t)$  corresponds to the sloping phases of the condensates of layer  $n$ . Assuming that  $q_n = q_0 \exp(i\omega t - nk_z z_0)$  ( $q_n$  represents any one of the dynamical variables in layer  $n$  and  $k_z \rightarrow k$  for brevity afterwards), we obtain the following dispersion relations for the transverse modes:

$$\omega^2(k) = 1 + \frac{Na_d}{R_x^3 R_y R_z} \Lambda(N_c), \quad (20)$$

where

$$\Lambda(N_c) \equiv \sum_{|m|=1}^{N_c} [1 - \cos(mkz_0)]. \quad (21)$$

The above mode is analogous to an optical phonon mode in crystals to which  $\omega(k=0)$  corresponds to a in-phase mode, while  $\omega(k=\pi/z_0)$  corresponds to an out-phase mode for neighboring layers. These two special cases are illustrated in Fig. 3. It can be simply checked that  $\omega(k=0) = 1$ . That is, in-phase mode frequency is just  $\omega_x$ .

Moreover, if we include only the nearest-neighbors ( $N_c = 1$ ) for  $\Lambda$  in Eq. (21), out-of-phase mode  $\omega(k = \pi/z_0)$  will be exactly the same as  $\omega_o$  for the bilayer system [see Eq. (12)]. At the long-wavelength limit ( $kz_0 \ll 1$ ), one obtains

$$\omega^2(k) \simeq 1 + v^2(N_c)k^2, \quad (22)$$

where the square of phonon velocity

$$v^2(N_c) \equiv \frac{Na_d z_0^2}{R_x^3 R_y R_z} \sum_{|m|=1}^{N_c} m^2 G_m. \quad (23)$$

Thus  $v^2 \propto Na_d$  at the low- $k$  limit. Measurements of dispersion relations of the phonon modes thus can give direct information on the value of DDI.

In Fig. 4, we plot the dispersion relations of transverse phonon mode  $\omega$  with  $(Na_s, Na_d) = (0, 1)$  and  $(0.5, 1)$  respectively. The numbers used are based on assuming that number of  $^{52}\text{Cr}$  atoms in each layer is  $N = 400$ , magnetic length  $\ell$  is about  $1\mu\text{m}$ , and hence  $Na_d$  is about 1. The curves presented in Fig. 4 are obtained using a proper truncation number  $N_c$  leading to satisfactory converged results (see later). Moreover, we assume that  $sE_r = 300$  and  $z_0 = 0.7\ell$  and hence  $s$  is about 30, which is in the deep optical lattice regime. By minimizing the energy functional (17), we obtain that  $R_z/R \simeq 0.074$  and  $z_0/R_z \simeq 7.0$  for the  $(Na_s, Na_d) = (0, 1)$  case and  $R_z/R \simeq 0.061$  and  $z_0/R_z \simeq 7.0$  for the  $(Na_s, Na_d) = (0.5, 1)$  case. Inset of Fig. 4 shows the linear dependence of  $k^2$  on  $\omega^2$  at the long wavelength limit. The slope is equal to the square of phonon velocity,  $v^2(N_c)$ . When the curve of finite  $a_s$  is compared to that of  $a_s = 0$ , one sees that repulsive  $s$ -wave coupling  $a_s$  acts to suppress the phonon mode as well as the phonon velocity. While short-range  $a_s$  plays no role between neighboring layers, its repulsion actually increases the radii of condensate ( $R_x, R_y, R_z$ ) in each layer and consequently  $\Lambda(N_c)/R_x^3 R_y R_z$  becomes smaller. This indicates that  $\omega^2$  as well as the phonon velocity will be smaller.

Finally the behaviors of  $\Gamma(N_c)$ ,  $\Lambda(N_c)$ , and  $v^2(N_c)$  as the function of  $N_c$  are studied. It is important to first note that  $\Gamma(N_c)$ ,  $\Lambda(N_c)$ , and  $v^2(N_c)$  all exhibit the same converging behavior. In Fig. 5(a),  $\Gamma(N_c)$  is plotted as the function of  $N_c$  for fixed  $R_z = 0.1\ell$  and  $R = 1\ell$  and three choices of  $z_0 = 0.5\ell, 0.9\ell$ , and  $1.3\ell$ . It is seen clearly in Fig. 5(a) that  $\Gamma(N_c)$  converges at some value of  $N_c$  and the larger the  $z_0$  is, the smaller the  $N_c$  is for the converging result. To be more explicit, we define a critical value  $N_c^g$  of  $N_c$  such that

$$\frac{\Gamma(N_c^g) - \Gamma(N_c^g - 1)}{\Gamma(N_c^g)} \lesssim 10^{-3}. \quad (24)$$

In fact,  $N_c^g = 19$  and  $25$  respectively for the two curves in Fig. 4.

Fig. 5(b) plots  $N_c^g$  as a function of  $z_0/R$ . It is found that  $N_c^g$  depends only on the ratio of  $z_0/R$  regardless of the value of  $R_z$ . This occurs because for the current

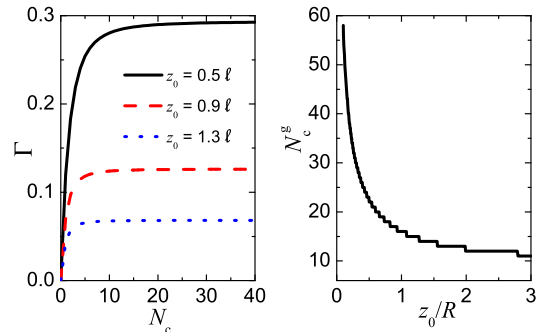


FIG. 5. (a)  $\Gamma(N_c)$  plotted as the function of  $N_c$  for three choices of  $z_0 = 0.5\ell, 0.9\ell$ , and  $1.3\ell$  and fixed  $R = 1\ell$  and  $R_z = 0.1\ell$ . (b) Critical number  $N_c^g$  (see text for definition) plotted as the function of  $z_0/R$ .

nonoverlapping multilayer system,  $R_z \ll z_0$  and  $R_z$  is no longer a well-defined length scale owing to the long-range character of DDI. As a matter of fact,  $N_c^g$  depends only on the ratio of  $z_0/R$ . When the ratio  $z_0/R$  is larger, the corresponding  $N_c^g$  is smaller and  $N_c^g \rightarrow 1$  in the limit of large  $z_0/R$ . The results of  $N_c^g$  indeed can help clarifying whether our results of transverse phonon modes are trustworthy or not. How does it work? Let us consider in a real experiment that total number of layers is  $N_s = 100$  and the ratio  $z_0/R$  is about 1. According to the results of Fig. 5(b),  $N_c^g = 16$  for  $z_0/R = 1$ . In this case, one does meet the criterion  $N_c \ll N_s$  and our results of transverse phonon modes are trustworthy when a real experimental measurement is compared to.

## V. CONCLUSIONS

In this paper, analytical solutions of mode frequencies for the motions of the center of condensates are studied in bilayer and multilayer (quasi-1D optical lattice) stacks. In the bilayer, it is shown that while DDI plays no role in the in-phase modes of center motions of condensates, out-of-phase modes ( $\omega_o$ ) depend crucially on the strength of DDI ( $a_d$ ). More explicitly,  $\omega_o$  will depend on condensate radii of each layer ( $R_x, R_y, R_z$ ), interlayer spacing ( $z_0$ ), as well as  $Na_d$ . Therefore one can actually extract the value of  $a_d$  if  $\omega_o$ , ( $R_x, R_y, R_z$ ), and  $z_0$  are measured experimentally. In the multilayer stack system, transverse (optical) phonon modes and phonon velocity are derived explicitly. Proper treatment was made for the boundary effect and it turns out that the truncation number to which how many neighboring sites should be included for the long-range DDI is a function of  $z_0/R$  ( $R$  is the condensate radius in the transverse direction) only.

## ACKNOWLEDGMENTS

We are grateful to the support of National Science Council (Grant No.: NSC 96-2112-M-003-008-MY3) and National Center for Theoretical Sciences, Taiwan.

- 
- [1] A. Griesmaier, J. Werner, S. Hensler, J. Stuhler, and T. Pfau, *Phys. Rev. Lett.* **94**, 160401 (2005).
- [2] K.-K. Ni, *et al.*, *Science* **322**, 231 (2008).
- [3] S. Ospelkaus, *et al.*, *Nature Phys.* **4**, 622 (2008).
- [4] R. M. Wilson, S. Ronen, J. L. Bohn, and H. Pu, *Phys. Rev. Lett.* **100**, 245302 (2008).
- [5] S. Ronen, D. C. E. Bortolotti, and J. L. Bohn, *Phys. Rev. Lett.* **98**, 030406 (2007).
- [6] O. Dutta and P. Meystre, *Phys. Rev. A* **75**, 053604 (2007).
- [7] N. G. Parker, C. Ticknor, A. M. Martin, and D. H. J. O'Dell, *Phys. Rev. A* **79**, 013617 (2009).
- [8] T. Koch, T. Lahaye, J. Metz, B. Fröhlich, A. Griesmaier, and T. Pfau, *Nat. Phys.* **4**, 218 (2008).
- [9] T. Lahaye, J. Metz, B. Fröhlich, T. Koch, M. Meister, A. Griesmaier, T. Pfau, H. Saito, Y. Kawaguchi, and M. Ueda, *Phys. Rev. Lett.* **101**, 080401 (2008).
- [10] L. Santos, G. V. Shlyapnikov, P. Zoller, and M. Lewenstein, *Phys. Rev. Lett.* **85**, 1791 (2000).
- [11] R. M. Wilson, S. Ronen, and J. L. Bohn, *Phys. Rev. A* **79**, 013621 (2009).
- [12] R. M. W. van Bijnen, D. H. J. O'Dell, N. G. Parker, and A. M. Martin, *Phys. Rev. Lett.* **98**, 150401 (2007).
- [13] J. Zhang and H. Zhai, *Phys. Rev. Lett.* **95**, 200403 (2005).
- [14] I. Tikhonenkov, B. A. Malomed, and A. Vardi, *Phys. Rev. Lett.* **100**, 090406 (2008).
- [15] P. Köberle and G. Wunner, *Phys. Rev. A* **80**, 063601 (2009).
- [16] M. Klawunn and L. Santos, *Phys. Rev. A* **80**, 013611 (2009).
- [17] R. Nath, P. Pedri, and L. Santos, *Phys. Rev. A* **76**, 013606 (2007).
- [18] A. Argüelles and L. Santos, *Phys. Rev. A* **75**, 053613 (2007).
- [19] D.-W. Wang, M. D. Lukin, and E. Demler, *Phys. Rev. Lett.* **97**, 180413 (2006).
- [20] V. M. Pérez-García, H. Michinel, J. I. Cirac, M. Lewenstein, and P. Zoller, *Phys. Rev. Lett.* **77**, 5320 (1996).
- [21] V. M. Pérez-García, H. Michinel, J. I. Cirac, M. Lewenstein, and P. Zoller, *Phys. Rev. A* **56**, 1424 (1997).
- [22] M. Albiez, R. Gati, J. Fölling, S. Hunsmann, M. Cristiani, and M. K. Oberthaler, *Phys. Rev. Lett.* **95**, 010402 (2005).
- [23] M. R. Andrews, C. G. Townsend, H.-J. Miesner, D. S. Durfee, D. M. Kurn, and W. Ketterle, *Science* **275**, 637 (1997).
- [24] S. Ronen, D. C. E. Bortolotti, and J. L. Bohn, *Phys. Rev. A* **74**, 013623 (2006).
- [25] Z. Hadzibabic, *et al.*, *Nature (London)* **441**, 1118 (2006).